Principles of Parallel Transmission

Peter Börnert and Ulrich Katscher
Philips Research Laboratories, Roentgenstrasse 24-26, D-22335 Hamburg, Germany
Peter.Boernert@.philips.com

Introduction

More than a decade ago, the multiple receive coil concept (1,2) has been introduced to improve the signal-to-noise-ratio (SNR) and, as suggested rather early, to shorten the acquisition times. This approach is nowadays called "parallel imaging", comprising the ideas of scan acceleration (3,4) and optimal coil-signal combination (2) and image uniformity correction (2).

Equivalent to the development of parallel imaging, multiple transmit coils have been proposed to perform "parallel transmission". The idea was triggered by the introduction of human high field proton MR systems, which showed B_1 uniformity problems caused by dielectric resonance effects. Thus, multi-port excitation for birdcage-type coils was proposed as a measure to improve the RF homogeneity in the excited volume (5,6). The underlying hardware could basically be considered as a multi-element transmit coil array, which allows changing the phase and amplitude of the otherwise identical RF waveforms for the individual ports. Meanwhile the basic feasibility of this RF shimming concept has been shown (7-10).

Triggered by these hardware developments and based on the analogy between RF pulse design and MR imaging (11,12), the principles of parallel imaging have recently been applied to RF transmission (13,14). Thus, RF pulses were proposed that are controlled by completely different time-courses in the individual transmit channels. This degree of freedom offers the possibility to improve spatially selective multi-dimensional RF pulses by, e.g., shortening the pulse duration, enhancing their spatial definition, or reducing their required RF power. Potential applications are: volume selective excitation (11,15,16) including outer volume signal suppression, curved slice imaging (17), or navigators employed for motion sensing (18). Furthermore, parallel transmission might ease the application of 3D RF pulses (19,20), which are limited by the finite lifetime of the transverse magnetization and the main field homogeneity. However, the compensation of patient induced RF inhomogeneities seems to emerge as a major application (21,22), particularly at high fields.

This paper outlines the basic principle of parallel transmission with the special focus on RF pulse shortening. Basic aspects, initial experimental proofs, the role of noise error propagation and some considerations on coil design will be discussed.

Theory

In parallel MR imaging, k-space is often undersampled, while data acquisition is performed with a number of individual receive coils. The potentially resulting image artifact is avoided by taking the coil sensitivity information during image reconstruction into account. Consequently, the central question in parallel imaging might be formulated as: given a couple of measured, e.g. undersampled data sets from individual coils, how does one get a single, entire image? This question has been answered so far by Roemer(2), Sodickson (3) and Pruessmann (4).

In analogy, in parallel transmission, each individual transmit coil could excite a specific magnetization pattern that could show artifacts, for example caused by subsampling of the excitation k-space or B_1 non-uniformities. However, their parallel superposition should result in the desired artifact-free magnetization pattern. Thus, the question is: which spatial patterns $P_i(\mathbf{r})$, that could show undersampling effects, have to be excited by each of the N transmit coils, each exhibiting a characteristic sensitivity profile $S_i(\mathbf{r})$, to obtain the desired excitation pattern $P_{des}(\mathbf{r})$? This constraint leads to Eq.[1], which turns out to be the central equation of parallel transmission:

$$P_{des}(\mathbf{r}) = \sum_{i=1}^{N} S_i(\mathbf{r})\ P_i(\mathbf{r}) \qquad [1]$$

Here, $P_{des}(\mathbf{r})$ is defined within the field of excitation (FoX), given on M spatial positions in a one-, two- or three-dimensional array. Equation [1] is linear and states that the superposition of all the individual pulse profiles $P_i(\mathbf{r})$, weighted by the corresponding (complex) coil sensitivity profiles, should yield the desired excitation pattern. It is assumed, that the $S_i(\mathbf{r})$ are known by means of B_1 mapping

techniques (23-25). If the transmit coils can be used in the receive mode, methods known from parallel imaging can be employed, assuming the reciprocal principle holds (4). To derive the unknown RF waveforms $B_{1i}(t)$ for the N individual transmit coil elements from Eq.[1], the following three steps have to be performed.

(A) Equation [1] has to be transformed into the Fourier domain (the excitation k-space). Thus, instead of the unknown $P_i(\mathbf{r})$ given in Eq.[1], now the equation contains the unknown $p_i(\mathbf{k})$:

$$p_{des}(\mathbf{k}) = \sum_{i=1}^{N} s_i(\mathbf{k}) \otimes p_i(\mathbf{k}) \qquad [2]$$

This step is performed because the B_1 waveform that excites a desired magnetization pattern is just its Fourier transform sampled along the chosen excitation k-space trajectory multiplied by some trajectory dependent weighting coefficients. This is according to Pauly's RF pulse design concept (11) based on the low tip angle approximation, which might hold for even higher flip angles (26) for special k-space trajectories.

In a slightly different writing of Eq.[2] as given in ref. (27), only the $P_i(\mathbf{r})$ in Eq. [1] is transformed to the Fourier domain, introducing the Fourier encoding matrix ($A \sim \exp(i\mathbf{rk})$):

$$P_{des}(\mathbf{r}) = \sum_{i=1}^{N} S_i(\mathbf{r})\, A(\mathbf{r},\mathbf{k})\, p_i(\mathbf{k}) \qquad [3]$$

This specific approach eases, e.g., the restriction of the excitation pattern $P_{des}(\mathbf{r})$ to a finite area inside the FoX.

(B) To separate the wanted $p_i(\mathbf{k})$, Eq.[2] has to be "inverted", which is nontrivial in case of an arbitrary k-space trajectory. To facilitate inversion, the k-space transformed coil sensitivities $s_i(\mathbf{k})$ are grouped into a single, "invertible" sensitivity matrix s_{full}. Additionally a corresponding single vector p_{full} is formed from the individual $p_i(\mathbf{k})$:

$$p_{des}(\mathbf{k}) = s_{full}(\mathbf{k})\, p_{full}(\mathbf{k}) \qquad [4]$$

Then, this re-formulated equation can be solved using the pseudoinverse, which is the optimal solution in the least square sense:

$$p_{full} = s_{full}^{H} \left(s_{full}\, s_{full}^{H} \right)^{-1} p_{des} \qquad [5]$$

The individual excitation patterns $p_i(\mathbf{k})$ can be extracted from p_{full}, which represents the general solution without any constraints. The separation of the $p_i(\mathbf{k})$ starting from Eq.[3] instead of Eq.[2] can be performed in an analog way.

Now the special case of a Cartesian, echo-planar like k-space trajectory, which is uniformly under-sampled in one dimension, is considered. Consequently, in the spatial domain only a limited number of voxels account for folding, which is described by the corresponding point spread function of the sampling scheme. As known from parallel imaging, this special case can be solved in the spatial domain (4) and leads to a small size of the sensitivity matrix to be inverted. This approach was chosen by Zhu (14) where the solution for the $p_i(\mathbf{k})$ is written as an integral over the FoX:

$$p_i(\mathbf{k}) = \int_{FoX} h_i(\mathbf{r}) P_{des}(\mathbf{r}) e^{-i\,2\pi\,kx} d\mathbf{r} \qquad [6]$$

In this equation, the h_i are derived from the inversion of a sensitivity matrix $C(S_1(\mathbf{r}), S_2(\mathbf{r}), \ldots, S_N(\mathbf{r}))$ described in ref. (14). The inversion of this sensitivity matrix C is the central step of the approach and might be compared with the inversion of the matrix s_{full} (Eq.[4]). Both matrices s_{full} and C depend solely on the spatial sensitivity distributions S_i, but differ in their detailed definitions (13,14).

(C) Once the $p_i(\mathbf{k})$ are calculated via Eq.[5] or [6], the mapping between **k** and t according to the chosen k-space trajectory has to be performed. This yields the actual B_1 waveforms applied in the time domain. The weighting function W(t) reflects the k-space sampling density, which is constant for Cartesian trajectories and takes the k-space velocity (the actual gradient) into account (11). The wanted waveforms can be calculated for each individual coil via:

$$B_{1i}(t) = W(t)\, p_i(\mathbf{k}(t)) \qquad [7]$$

The resulting degree of freedom introduced by the use of multiple transmit coils can be exploited in several directions. A major application is given by the reduction of the pulse duration by a factor R, corresponding to the reduction of acquisition time in parallel imaging. Instead of reducing the pulse duration, the spatial definition of the excitation pattern can be increased without changing the pulse duration. Furthermore, system imperfections like B_0 inhomogeneities, k-space trajectory imperfections, concomitant gradients effects, etc. can be compensated for (12,28).

A further interesting opportunity of using multiple transmit coils is to reduce the required RF power, and thus, the specific energy absorption rate (SAR) (13,29,30-32). The intrinsic freedom in solving Eq.[4] can be used to favors those solutions which exhibit the lowest RF power.

As mentioned above, a different form of parallel transmission is performed for the purpose of RF shimming, which is desirable especially for high field applications. Here, the amplitudes A_i and phases ϕ_i of the otherwise identical B_1 waveforms are adjusted for the different transmit array elements to yield optimal spatial excitation homogeneity (5-7). This is also described by Eq. [1]. The optimum A_i and ϕ_i can be derived if the individual excitation pattern $P_i(\mathbf{r})$ are replaced by constant weighting factors $F_i = A_i \exp(i\phi_i)$, which are spatially invariant. In this case, Eq. [1] can be solved for the F_i via a matrix inversion in the spatial domain choosing a constant $P_{des}(\mathbf{r})$. Obviously, a non-constant $P_{des}(\mathbf{r})$ might be chosen in this framework as well.

Experimental Proof

The theoretical development of parallel transmission preceded the corresponding experimental abilities by several years. However, experimental proofs of the basic principles have been realized using some work-arounds (13,14). Thus, parallel transmission was mimicked in sequential experiments using different transmit coils and making use of the linearity of the problem (c.f. Eq.[1]) by averaging their results after signal acquisition (Fig.1).

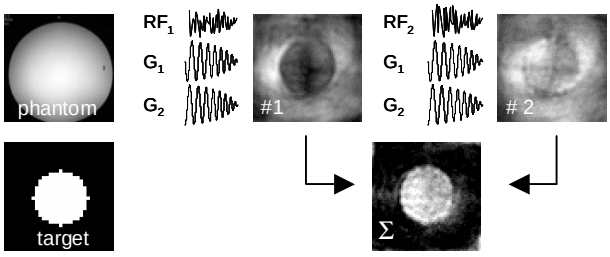

Fig. 1. Parallel transmission - proof of principle (13). In a phantom experiment two different pre-defined 2D RF pulses (RF_1, RF_2) were applied, each with a different transmit coil using the same sub-sampled spiral k-trajectory. Artefacts are visible. After signal summation the desired target magnetisation pattern is obtained.

With the development of multi-element-transmit coils (33-35), parallel transmission has been used to perform RF shimming (7-10) by varying amplitudes and phases for the individual channels. However, a full verification of the entire concept was accomplished by the introduction of prototype MR systems (36,10) which allowed driving the RF waveform individually for each channel. Thus, spatially selective 2D RF pulses, using different k-space trajectories, have been considerably accelerated (34,10).

Error Propagation

Noise that might degrade the performance of parallel transmission might originate from, e.g., the D/A converting process and RF amplifier imperfections. This system noise affects the individual pulse profiles $P_i(\mathbf{r})$, and thus, influences the final result in a linear way as a superposition in the spatial domain (cf. Eq.[1]). Errors in the coil sensitivity profiles caused by noise or measurement imperfections also influence the final result linearly via Eq.[1]. It is important to note that the system noise does not interact with the central matrix inversion (see e.g., Eq.[5]). This is a crucial difference with respect to parallel imaging, where the system noise generated in the receive chain is enhanced if the matrix inversion is ill conditioned (4). In parallel imaging, the inverted matrix is multiplied with the measured data bearing noise. In parallel transmission, the inverted matrix is multiplied with the desired excitation pattern, which is free of noise (see Fig.2).

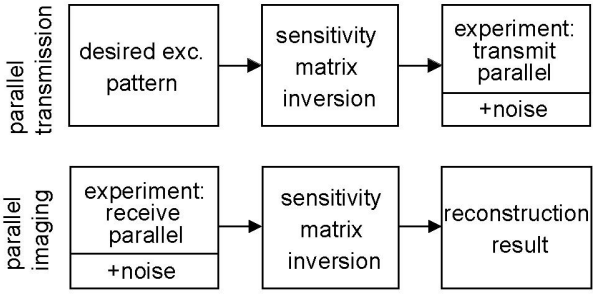

Fig. 2. Schematic comparison of parallel transmission and parallel imaging. Experimental noise comes into play after / before the inversion of the sensitivity matrix, which leads to a larger robustness of parallel transmission than parallel imaging.

In that respect, the concept of the geometry factor as deduced for parallel imaging (4) cannot be adapted directly to parallel transmission.

If the inverse problem of parallel transmission is ill posed, the superposition of Eq.[1] does not lead to a complete cancellation of the subsampling artifacts, and noise-like aliasing structures appear in the final result. The problem becomes ill posed if the spatial frequency components of the actual coil sensitivity profiles are not able to compensate for the missing parts of a reduced k-space trajectory. Thus, a proper interplay between the coil sensitivity profiles and the involved trajectories has to be found. From this

interplay, conditions for the sensitivity profiles, and thus, the used coil array can be derived.

Coil design and SAR aspects

It is important to know how sensitive the RF pulse performance depends on the transmit coil array geometry. Due to the different error propagation behavior compared to parallel imaging, parallel transmission should be less sensitive. This was confirmed recently by corresponding simulations, which showed that RF pulse performance is in general rather robust (37) against variations of the transmit coil array configuration and becomes critical only for very artificial cases.

On the other hand, if the sensitivity matrix s_{full} to be inverted becomes ill posed, the norm of the resulting vector p_{full}, containing the RF waveforms, may increase (c.f. Eq.[4]). This increase would lead to an increase of the required RF power and the SAR, respectively. Thus, SAR could serve as an important coil design criterion. However, it has been found, that the RF pulse performance proves to be fairly stable (37,38) and thus, the question of an ill posed inverse problem plays only a minor role in parallel transmission. This gives rise to a much larger freedom in designing coil arrays for parallel transmission than for parallel imaging.

Summary

Parallel transmission follows the development of parallel imaging. Parallel transmission can be used to shorten the duration of spatially selective RF pulses or to increase their spatial resolution definition maintaining the pulse duration. Other applications envisaged might be the reduction of the required RF power, i.e. the SAR, or RF shimming. In parallel imaging and transmission it is necessary to determine and invert a matrix derived from the spatial sensitivities of the coils involved. However, parallel transmission is not just the reciprocal version of parallel imaging. As a consequence of this asymmetry, it seems that the error propagation in parallel transmission does not lead to pronounced non-linear effects as in parallel imaging, described by the geometry factor.

Very likely, future standard high-field MR systems will be capable of parallel transmission. These MR systems will be able to improve RF pulse performance in many respects, thus opening a wide range of new and exciting applications.

References

1. Hyde JS, Jesmanowicz A, Froncisz W, Kneeland JC, Grist TM. Parallel image acquisition from noninteracting local coils. J. Magn. Reson. 1986; 70: 512-517.
2. Roemer PB, Edelstein WA, Hayes CE, Souza SP, Mueller OM. The NMR phased array. Magn. Reson. Med. 1990; 16: 192-225.
3. Sodickson DK, Manning WJ. Simultaneous acquisition of spatial harmonics (SMASH): fast imaging with radiofrequency coil arrays. Magn. Reson. Med. 1997; 38: 591-603.
4. Pruessmann KP, Weiger M, Scheidegger MB, Boesiger P. SENSE: sensitivity encoding for fast MRI. Magn. Reson. Med. 1999; 42: 952-962.
5. Sotgiu A, Hyde JS. High-order coils as transmitters for NMR imaging. Magn Reson. Med. 1986; 3: 55-62.
6. Ibrahim TS, Lee R, Baertlein BA, Kangarlu A, Robitaille PL. Application of finite difference time domain method for the design of birdcage RF head coils using multi-port excitations. Magn. Reson. Imag. 2000; 18: 733-742.
7. Seifert F, Rinneberg H. Adaptive coil control: SNR optimization of a TR volume coil for single voxel MRS at 3 T. Proc. Intl. Soc. Mag. Reson. Med. 2002; 10: 162.
8. Adriany G, Van de Moortele PF, Wiesinger F, Moeller S, Strupp JP, Andersen P, Snyder C, Zhang X, Chen W, Pruessmann KP, Boesiger P, Vaughan T, Ugurbil K. Transmit and receive transmission line arrays for 7 Tesla parallel imaging. Magn. Reson. Med. 2005; 53: 434-45.
9. Zhu Y, Giaquinto R. Improving Flip Angle Uniformity with Parallel Excitation. Proc. Int. Soc. Magn. Reson. Med. 2005; 13: 2752.
10. Ullmann P, Junge S, Wick M, Seifert F, Ruhm W, Hennig J. Experimental analysis of parallel excitation using dedicated coil setups and simultaneous RF transmission on multiple channels. Magn. Reson. Med. 2005; 54: 994-1001.
11. Pauly J, Nishimura D, Macovski A. A k-space analysis of small-tip-angle excitation. J. Magn. Reson. 1989; 81: 43-56.
12. Börnert P, Aldefeld B. On spatially selective RF excitation and its analogy with spiral MR image acquisition. MAGMA, 1998; 7: 166-178.
13. Katscher U, Börnert P, Leussler C, van den Brink J. Transmit SENSE. Magn. Reson. Med. 2003; 49: 144-150.
14. Zhu Y. Parallel excitation with an array of transmit coils. Magn. Reson. Med. 2004; 51: 775-784.
15. Hardy VJ, Cline HE. Spatial localization in two dimensions using NMR designer pulses. J. Magn. Reson. 1989; 82: 647-654.
16. Bottomley PA, Hardy CJ. Progress in efficient 3-dimensional spatially localized in vivo P-31 NMR-spectroscopy using multidimensional spatially selective (Rho) pulses. J Magn Reson 1987; 74: 550-556.

17. Börnert P, Schäffter T. Curved slice imaging. Magn. Reson. Med. 1996; 36: 932-939.
18. Sachs TS, Meyer CH, Hu BS, Kohli J, Nishimura D, Macovski A. Real-time motion detection in spiral MRI using navigators. Magn. Reson. Med. 1994; 32: 639-645.
19. Pauly JM, Hu BS, Wang SJ, Nishimura DG, Marcovski A. A three-dimensional spin-echo or inversion pulse. Magn. Reson. Med. 1993; 29: 2-6.
20. Wong ST, Roos MS. A strategy for sampling on a sphere applied to 3D selective RF pulse design. Magn. Reson. Med. 1994; 32: 778-784.
21. Saekho S, Boada FE, Noll DC, Stenger VA. Small tip angle three-dimensional tailored radiofrequency slab-select pulse for reduced B1 inhomogeneity at 3 T. Magn. Reson. Med. 2005; 53: 479-84.
22. Ulloa JL, Irarrazaval P, Hajnal JV. Exploring 3D RF shimming for slice selective imaging. Proc. Intl. Soc. Mag. Reson. Med. 2005; 13: 21.
23. Glover GH, Hayes CE, Pelc NJ, Edelstein WA, Mueller OM, Hart HR, Hardy CJ, O'Donnell M, Barber WD. Comparison of Linear and Circular Polarization for Magnetic Resonance Imaging. J. Magn. Reson. 1985; 64: 255-270.
24. Barker GJ, Simmons A, Arridge SR, Tofts PS. A simple method for investigating the effects of non-uniformity of radiofrequency transmission and radiofrequency reception in MRI. Brit. J. Radiol. 1998; 71: 59-67.
25. Griswold MA, Kannengiesser S, Müller M, Jakob PM. Autocalibrated Accelerated Parallel Excitation (Transmit-GRAPPA). Proc. Int. Soc. Magn. Reson. Med. 2005; 13: 2435.
26. Pauly J, Nishimura D, Macovski A. A linear class of large-tip-angle selective excitation pulses. J. Magn. Reson. 1989; 82: 571-587.
27. Grissom WA, Yip CY, Noll DC, An Image Domain Approach for the Design of RF Pulses in Transmit SENSE, Proc. Int. Soc. Magn. Reson. Med. 2005; 13: 19.
28. Yip CY, Fessler JA, Noll DC. A novel, fast and adaptive trajectory in three-dimensional excitation k-space. Proc. Intl. Soc. Mag. Reson. Med. 2005; 13: 2350.
29. Conolly S, Nishimura DG, Macovski A, Glover G. Variable-rate selective excitation. J. Magn. Reson. 1988; 78: 440–458.
30. Graesslin I, Niemann M, Harvey P, Vernickel P, Katscher U. SAR and RF Power Reduction with Parallel Excitation using Non-Cartesian Trajectories. MAGMA 2005; 18: S251
31. Katscher U, Börnert P, van den Brink, JS. Theoretical and Numerical Aspects of Transmit SENSE. IEEE Trans. Med. Imag. 2004; 23: 520-525.
32. Yip CY, Fessler JA, Noll DC. Iterative RF pulse design for multidimensional, small-tip-angle selective excitation. Magn. Reson. Med. 2005; 54: 908-917.
33. Boskamp E, Lee RF. Whole Body LPSA tranceive array, Proc. Int. Soc. Magn. Reson. Med. 2002; 10: 903.
34. Weyers D, Boskamp E. An 8 channel volume transmit coil, Proc. Int. Soc. Magn. Reson. Med. 2002; 10: 901.
35. Lee RF, Giaquinto RO, Hardy CJ. Coupling and decoupling theory and its application to the MRI phased array. Magn. Reson. Med. 2002; 48: 203-213.
36. Zhu Y, Watkins R, Giaquinto R, Hardy C, Kenwood G, Mathias S, Valent T, Denzin M, Hopkins J, Peterson W, Mock B. Parallel Excitation on an Eight Transmit-Channel MRI System. Proc. Int. Soc. Magn. Reson. Med. 2005; 13: 14.
37. Katscher U, Röhrs J, Börnert P. Basic considerations on the impact of the coil array on the performance of Transmit SENSE. MAGMA 2005; 18: 81-88.
38. Katscher U, Vernickel P, Overweg J. Basics of RF Power Behaviour in Parallel Transmission. Proc. Int. Soc. Magn. Reson. Med. 2005; 13: 17.